

BEHAVIOR OF LIGHTWEIGHT AGGREGATE CONCRETE FILLED STEEL TUBULAR SLENDER COLUMNS UNDER AXIAL COMPRESSION

Fu Zhong-qiu ¹, Ji Bo-hai ^{2,*}, Lv Lei ³ and Zhou Wen-jie ³

¹PhD Candidate, College of Civil and Transportation Engineering
Hohai University, Xikang Road 1#, Nanjing, Jiangsu, P.R. China 210098

²Professor, College of Civil and Transportation Engineering
Hohai University, Xikang Road 1#, Nanjing, Jiangsu, P.R. China 210098

³M.E., College of Civil and Transportation Engineering
Hohai University, Xikang Road 1#, Nanjing, Jiangsu, P.R. China 210098

*(Corresponding author: E-mail: hhbhji@163.com)

Received: 11 July 2010; Revised: 28 September 2010; Accepted: 23 November 2010

ABSTRACT: Based on axially compressive tests on 6 short columns and 27 slender columns of lightweight aggregate concrete filled steel tube (LACFST), macroscopic deformation characters, axial force-longitudinal strain curves, failure mode and failure mechanism are studied. The results are also compared with these of the normal concrete filled steel tube. The test results demonstrated that slenderness ratio is the main influence factor to the behavior of LACFST long columns under axial load. The greater the slenderness ratio is, the lower the ultimate bearing capacity and stability coefficient of the specimen are, and the performances of core concrete affect the stability behavior of lightweight aggregate concrete and normal concrete filled steel tube long columns. The stability coefficient of specimens is determined by the peak strain of concrete and unrelated to the peak strength of concrete. The stability coefficient increases when the peak strain of concrete increasing. Comparison results show that calculation formula in Europe code EC4 (1996) can be applied to calculate the bearing capacity of LACFST columns under axially compressive load.

Keywords: Lightweight aggregate concrete filled steel tube; axial compressed test; slenderness ratio; stability coefficient; bearing capacity

1. INTRODUCTION

Modern structure requires high strength and light materials. Concrete filled steel tube (CFST) exploits the advantages of the steel tensile properties and concrete compressive properties. The concrete can delay the local buckling of steel pipe, and steel tube confined concrete increase its compressive strength. Compare to concrete structures, component section of CFST is smaller which greatly reduces self-weight and have good seismic performance [1]. And the construction is simple without complicated pre-stress tensioning. Currently, the properties of CFST had been studied by many researchers [2, 3, 4], and norms were made in different countries [5]. It is used in building and bridge structures [6, 7, 8].

Lightweight aggregate concrete (LAC) has advantages of higher strength/weight ratio, thermal insulation and fire resistance characteristics, without alkali-aggregate reaction [9]. LAC is about 20% to 30% lighter than normal concrete. Its thermal conductivity is about 12% to 33% of the normal one. At the same time, it is an environmentally and friendly material. Existing research shows that lightweight concrete also has good mechanical properties [10]. But Compare to normal concrete, LAC has a lower elastic modulus and higher brittleness. If lightweight aggregate concrete is used to fill steel tube, it forms lightweight aggregate concrete filled steel tube (LACFST). Because of the restraint of steel, the strength and brittleness can be improved. And using LACFST in structural can reduce weight. Especially in the long span bridge and high-rise building structures, the application of LACFST can reduce the cost.

Lightweight aggregate concrete is one of the future development directions of concrete application. This provides application possibility of LACFST in future. Japan has successfully used LACFST in "Shinkansen" project (high-speed railway bridge) [11]. But according to the published literature [12], it shows that the study about the performance of LACFST is still in a primary stage. In this study results of the axial compression test of 33 short and slender LACFST specimens are presented, and the performance of LACFST slender columns is discussed.

2. EXPERIMENTAL INVESTIGATIONS

2.1 Materials

The coarse aggregate of the lightweight aggregate concrete used in the test is shale ceramic with physical and mechanical properties as follows: Lightweight aggregate of bulk density is 814kg/m^3 , cylindrical compressive strength is 8.5MPa and water absorption ratio is 6% an hour. Two different types of concrete using ordinary Portland cement and washed river sand were used in casting the specimens. The concrete mixture and material properties are shown in Table 1.

Table 1. Mixture of LAC Concrete (kg/m^3) and Material Properties

Cubic strength f_{cu} (MPa)	Prism strength f_{ck} (MPa)	Cement	Haydite	Sand	Mineral powder	Water	Water reducer	Elastic Modulus (GPa)
34.3	25.6	460	670	650	0	203	0	19.5
47.6	39.3	450	650	650	50	125	6.8	29.6

According to the relevant Chinese standards, compression tests were carried out on a number of Standard cubes ($[150 \times 150 \times 150]$ mm) to determine the concrete grade, and prisms ($[150 \times 150 \times 300]$ mm) in order to determine the 28-days compressive strength (f_{ck}) and elastic modulus (E_c) of the unconfined concrete.

Straight welded steel tube Q235 was used in the test. According to Chinese standard "Metallic materials at ambient temperature tensile test method" (GB/T228-2002) (2002) [13], tension tests on a group of three coupons were conducted to determine the tensile strength, where the thickness of each section of steel tube made into the interception of the standard specimen. The tension coupons were cut from the steel tube. The dimensions of the coupon are shown in Figure 1.

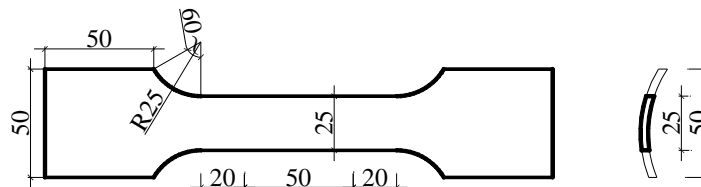


Figure1. Dimensions of the Tensile Coupons (mm)

Before tensile test, the ends of the specimen were compressed flatten to ensure it can be clamped and forced uniformly. Strain gauges were pasted on both sides of the coupon to measure the strain. The strain was collected by TS3890 pseudo-dynamic strain instrument in the whole process. From the relationship of stress and strain, the material properties are shown in Table 2.

Table 2. Material Properties of Steel

Thickness t (mm)	Yield strength f_y (MPa)	Poisson's ratio ν_s	Ultimate strength f_u (MPa)	Elastic Modulus E_s (MPa)
2.5	298.92	0.273	352	2.01×10^5
3.5	316.45	0.289	370	2.09×10^5

2.2 Specimens

Different slenderness ratio and concrete strength were considered. Two ends of the steel tubes were flat. Before pouring concrete, each column was welded with a 10 mm thick circular plate on one side. Its center is the same with the geometric center of the steel tube. The LAC was filled in layers; each layer was 500mm vibrated manually to ensure its density, and cured by natural conditions. Surface hollows due to concrete shrinkage were filled up with grout to confirm the specimen side smoothness. The parameters of LACFT specimens are given in Tables 3 together with the results to be discussed later.

2.3 Test Instruments and Procedure

The details of the test instruments are shown in Figure 2. The experiment was performed in the structural engineering laboratory of Hohai University. Hydraulic jack was implemented to apply loads on the specimens. Pressure sensor and resistance strain gauges were installed to measure loads and strains respectively. At the two ends of the specimens, column joint utilized to simulate the hinged boundary conditions.

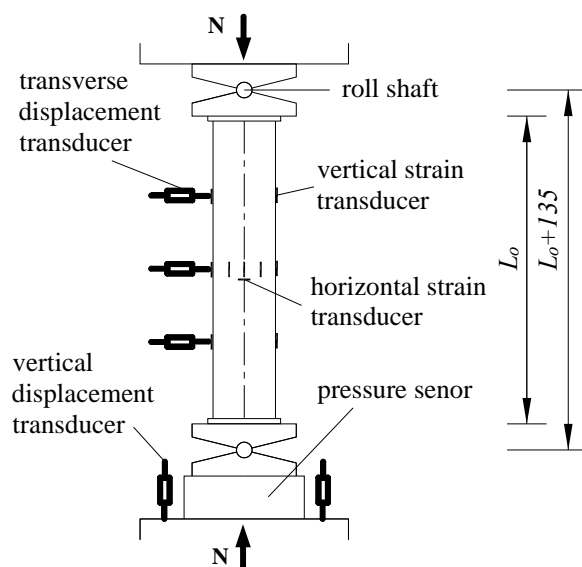


Figure 2. Loading and Measurement System

Table 3. Detail of the Test Specimens

Specimens	Pipe size (mm)			λ	f_{ck} (MPa)	f_y (MPa)	ξ	N_u (kN)	$\varphi=N_u/N_o$
	D	t	L_0						
SC1-3-a	165	2.5	495	12	25.6	298.92	0.74	948.57	1.0229
SC1-3-b	165	2.5	495	12	25.6	298.92	0.74	896.19	0.9665
SC1-3-c	165	2.5	495	12	25.6	298.92	0.74	937.14	1.0106
SC1-7-a	165	2.5	1155	31.2	25.6	298.92	0.74	793.33	0.8555
SC1-7-b	165	2.5	1155	31.2	25.6	298.92	0.74	753.33	0.8124
SC1-10-a	165	2.5	1650	43.2	25.6	298.92	0.74	798.10	0.8607
SC1-10-b	165	2.5	1650	43.2	25.6	298.92	0.74	713.33	0.7693
SC1-10-c	165	2.5	1650	43.2	25.6	298.92	0.74	736.19	0.7939
SC2-3-b	114	3.5	342	12	39.3	316.45	1.09	879.00	0.9903
SC2-3-c	114	3.5	342	12	39.3	316.45	1.09	896.19	1.0097
SC2-7-a	114	3.5	798	32.8	39.3	316.45	1.09	799.05	0.9002
SC2-7-b	114	3.5	798	32.8	39.3	316.45	1.09	698.10	0.7865
SC2-10-a	114	3.5	1140	44.8	39.3	316.45	1.09	797.14	0.8981
SC2-10-c	114	3.5	1140	44.8	39.3	316.45	1.09	800.00	0.9013
SC2-14-a	114	3.5	1596	60.8	39.3	316.45	1.09	824.76	0.9292
SC2-14-b	114	3.5	1596	60.8	39.3	316.45	1.09	770.48	0.8681
SC3-3-a	114	3.5	342	12	25.6	316.45	1.67	746.67	1.0056
SC3-3-b	114	3.5	342	12	25.6	316.45	1.67	712.38	0.9594
SC3-3-c	114	3.5	342	12	25.6	316.45	1.67	768.57	1.0351
SC3-7-a	114	3.5	798	32.8	25.6	316.45	1.67	584.76	0.7875
SC3-7-b	114	3.5	798	32.8	25.6	316.45	1.67	643.81	0.8670
SC3-7-c	114	3.5	798	32.8	25.6	316.45	1.67	652.38	0.8786
SC3-10-a	114	3.5	1140	44.8	25.6	316.45	1.67	603.81	0.8132
SC3-10-b	114	3.5	1140	44.8	25.6	316.45	1.67	598.10	0.8055
SC3-10-c	114	3.5	1140	44.8	25.6	316.45	1.67	581.90	0.7837
SC3-14-a	114	3.5	1596	60.8	25.6	316.45	1.67	548.57	0.7388
SC3-14-b	114	3.5	1596	60.8	25.6	316.45	1.67	541.90	0.7298
SC3-14-c	114	3.5	1596	60.8	25.6	316.45	1.67	529.52	0.7131

- Note: 1. D is the external diameter, t is the thickness, L_0 is the length of specimen, and calculation length is $L=L_0+135$;
2. f_{ck} is Prism strength of concrete, f_y is the yield strength of steel;
3. ξ is Confinement coefficient, $\xi=A_s f_y / (A_c f_{ck})$, here A_s is the area of steel, A_c is the area of concrete;
4. N_u is test ultimate load, N_0 is test ultimate load of short column;
5. λ is the slenderness ratio, $\lambda=4L/D$; φ is stability factor, $\varphi=N_u/N_0$.

For the accuracy of the specimen's deformation measurements, eight strain gauges were set at the mid-length of the column to record strain's values. Three displacement transducers were installed in the bending plane, the top and the bottom gauges were at distance of one fourth the height of each column from the top and the bottom, respectively, and the third displacement transducers was positioned at the mid-height of each column to measure the lateral deformation. In order to measure the portrait deformation two displacements transducers were set up. All these transducers were connected to computer data acquisition system to record their values in the whole test phases.

The specimens were loaded at rate of 1/10 of the predicted ultimate load in the elastic phase and at loading rate of 1/15 of the predicted ultimate load in the column yielding phase. Each load was maintained 2-3 minutes to enable the full deformation development. When approaching the predicted ultimate load, the load was added slowly.

3. DISCUSSIONS OF TEST RESULTS

3.1 Failure Process

Figure 3 shows the failure mode of two groups specimens. Figure 4 shows part of the load N – midpoint deflection f curves. The specimens are all destroyed because of excessive lateral deformation. At the beginning, the deflection of the specimen increases slowly as the load increases. When it was close to the ultimate bearing capacity, the lateral deformation enlarged quickly. After reaching the maximum value, the load began to decrease. With higher slenderness ratio of the specimen, the load decreased and the lateral deflection increased faster. Coupled local global buckling was also observed on some of small slenderness ratio specimens at ends and middle part (Figure 3(a)).



Figure 3. Failure specimens

From Figure 4, the lateral deflection developed gradually at the beginning of the loading process. After a period of elastic deformation, the curves go into plastic stage, and approaches to the ultimate load. Then the load decreases as the lateral deflection increases. The larger the slenderness ratio is, the quicker the decreasing speed of load is. The lateral deflection of some specimens increases at the beginning of the test. Because it is hard to make sure that the load was axial exactly, and the material is uneven, the specimens were imperfection initially. But some of the specimens also appeared perfect axial compression state (Figure 4 (a)).

Load (N) – middle point strain (ε_s) curves were shown in Figure 5. It reflects the changing process of lateral deflection when loading. Tensile one is the circumferential strain, and the compressive one is the longitudinal strain. Line a and b represents the strain curve of two points at different side of roll shaft. Point a is the lateral side of flexural specimen, and point b is the medial side of flexural specimen. The strain ε_s , including longitudinal strain and circumferential strain, was measured by resistance strain gauge externally bonded on the steel tube. At the beginning, the cross sections were compressed and the both sides strain were similar. With the load growth and the lateral deformation development, the differences of the strain on both sides increased until it reached the ultimate load. Because of the significant deformation, the larger slenderness ratio specimens damaged with one side subjected to tension and another side subjected to compression.

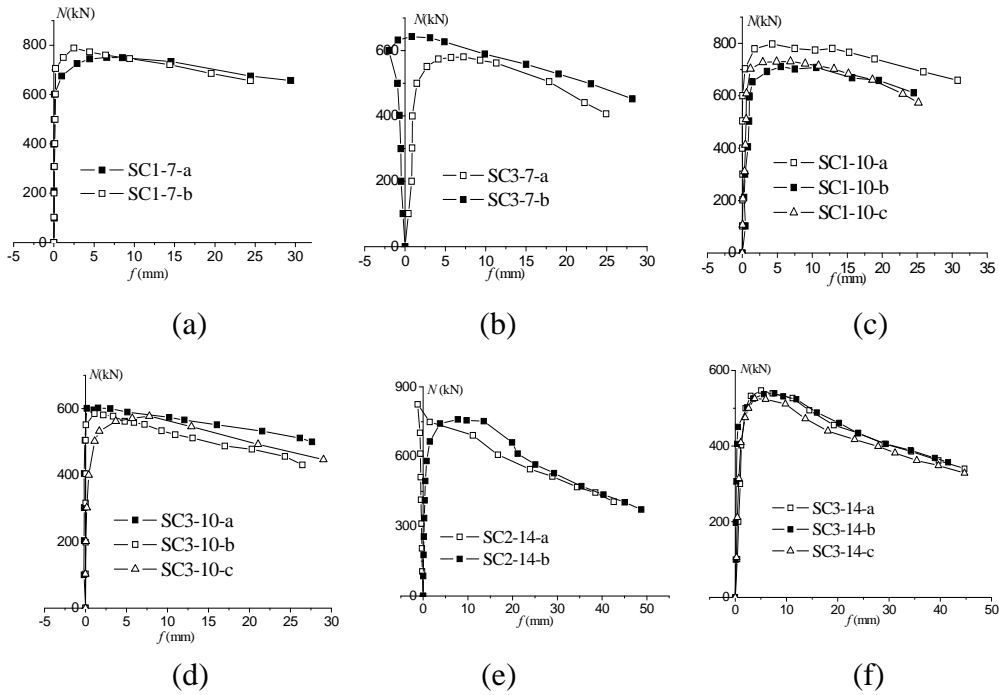


Figure 4. Load (N) – Midpoint Displacement (f) Curves

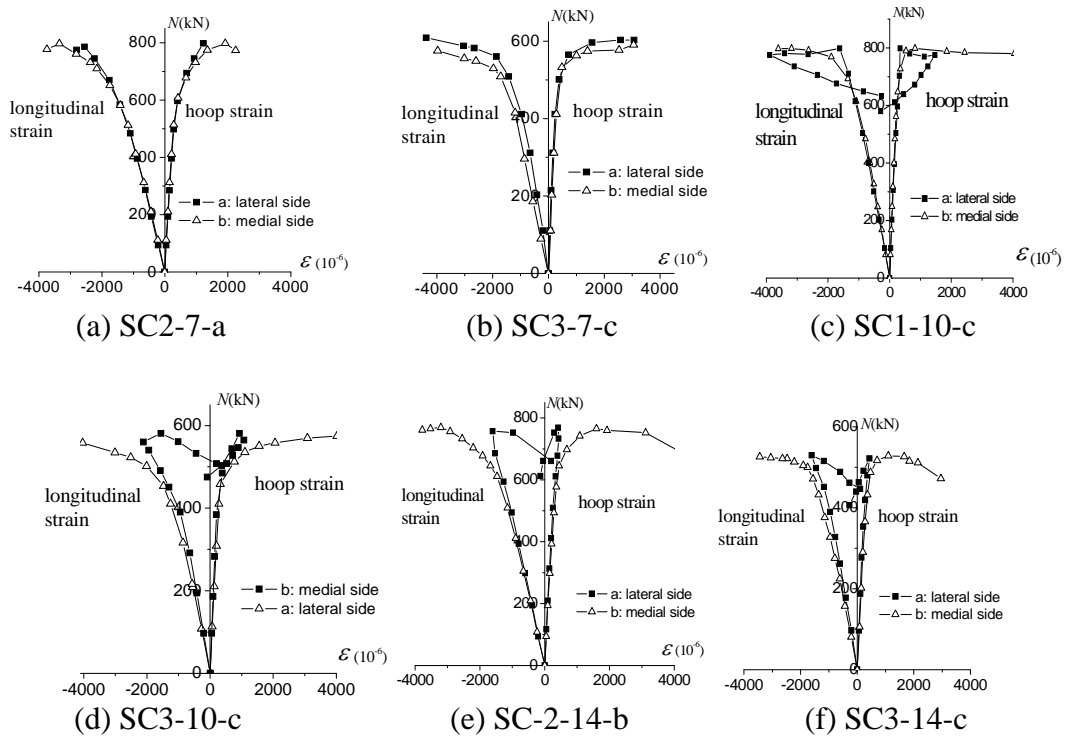


Figure 5. Load (N) – Middle Point Strain (ϵ_s) Curves

3.2 Failure Characteristics

The slenderness ratio is one of the important parameters of such test. Figure 6 shows the axial load N - longitudinal strain ε_c curves of the three groups specimens. The expression of ε_c is following one.

$$\varepsilon_c = \frac{\Delta}{L} \quad (1)$$

In the expression, Δ is the longitudinal compression displacement measured by displacement meters, L is the length of the specimen. From the N - ε_c curves in Figure 6, it can be found that the failure of specimens were all elastic-plastic damage with instability.

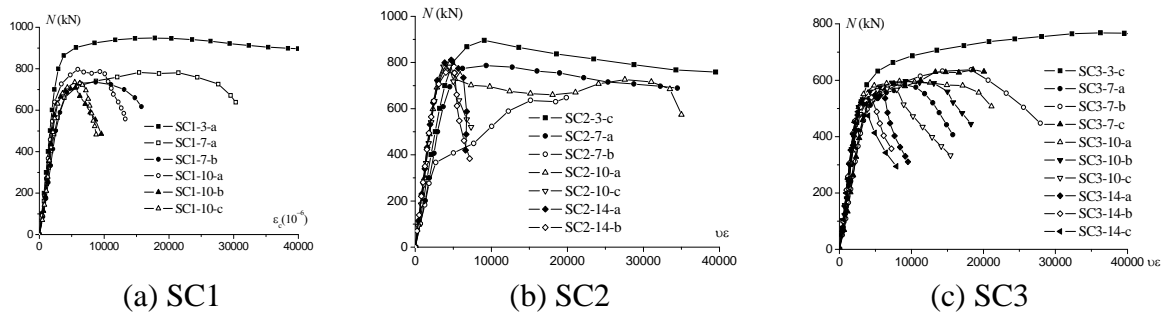


Figure 6. Load (N) - Longitudinal Strain(ε_c) Curves

Study on axial compression of short LACFST columns shows that it has good mechanical performance. So the N - ε_c curves of short column are drawn in Figure 6 to compare with the long columns. In the elastic stage, the N - ε_c curves of all the long column specimens are almost overlap with each other, and almost the same with curves of the short column. After reaching the elastic-plastic deformation stage, the N - ε_c curves with different slenderness ratios appear diversity between each other. With $L_o / D = 7$ (SC1-7, SC2-7, SC3-7) and $L_o / D = 10$ (SC1-10, SC2-10, SC3-10), the curves deviate from the original direction of elastic stage after the elastic limit. But the load grows slowly until to the ultimate load. After the ultimate load, the load decreases slowly, while the deformation increases quickly and the plastic deformation are obvious. With $L_o / D = 14$ (SC1-14, SC2-14, SC3-14), the curves have a shorter upward tendency and then fall down quickly after the elastic limit. The specimens almost lose bearing capacity suddenly. The N - ε_c curves of the long column specimens are lower than that of short column specimens in the figures. Compare to the short columns, the long ones have lower bearing capacity and the elastic-plastic stage occurs earlier. The long column specimens are instability damage because of large lateral deformation. They are elastic-plastic instability failure.

3.3 Failure Mechanism

The lateral deformation coefficient μ is defined similar as Poisson's ratio. It can be calculated by following equation.

$$\mu = \varepsilon_{sh} / \varepsilon_{sl} \quad (2)$$

ε_{sh} is the hoop strain and ε_{sl} is the longitudinal strain of the steel at middle point. They were measured by the strain gauges on the steel tube. It can reflect whether the material has yielded or not. Figure 7 is the lateral deformation coefficient variation curve of a group of specimens with different slenderness ratio. Poisson's ratio of steel is 0.25~0.3 usually. If the lateral deformation coefficient is less than 0.3, the steel tube is in elastic stage. At the beginning of loading, the lateral deformation coefficient is same to the Poisson's ratio of steel. The lateral deformation of concrete provides less extrusion effect to steel tube. While the lateral deformation coefficient is larger than 0.3, it produces interaction force between concrete and steel.

In Figure 7, after reaching the ultimate bearing capacity, the $\mu - N$ curves trend on medial side(b line) was similar with different slenderness ratios, while it was different on lateral sides(a line). Because the flexure of specimens with $L_o / D = 14$ (SC1-14, SC2-14, SC3-14), was obvious, the longitudinal stress on the lateral side changed from compression to tension (Figure 5). When the specimen with $L/D=14$ damaged, the lateral side was in elastic stage, while the medial side was in plastic stage. But for the specimens with smaller slenderness ratios, both sides were in plastic stage when damaged.

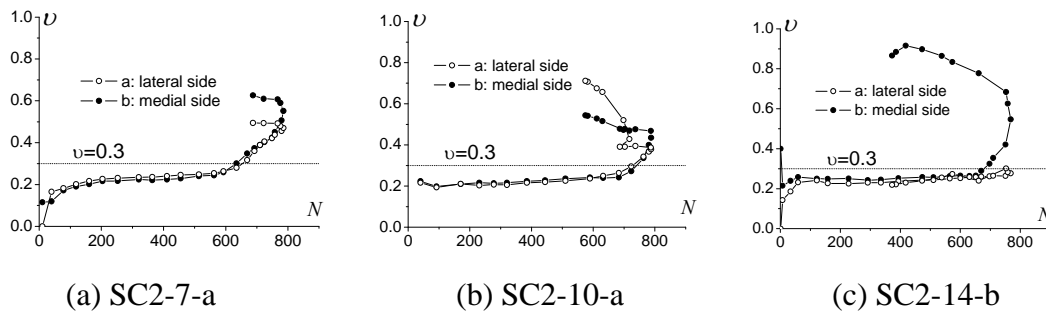


Figure 7. Lateral Deformation Coefficient (μ) - Load (N) Curves

3.4 Influence of Slenderness Ratio to Bearing Capacity

From the discussions above, it can be seen that the slenderness ratio influences the behavior of LACFST columns greatly. Generally, when columns have a larger slenderness ratio, the bearing capacity mainly depends on the slenderness ratio. Under the same axial force, the lateral deformation of specimens with large slenderness is greater. And it causes greater additional moment. This makes the columns have a lower bearing capacity. In this test, slenderness ratio is a controlling parameter. Through the $N - \varepsilon_c$ curves(Figure 6), it can be found that when the slenderness ratio is greater, the ultimate strength is lower and the plastic deformation is worse. It's same conclusion with other material columns.

4. STABILITY BEHAVIOR ANALYSIS

4.1 Parameters Influence to Stability Coefficient

Figure 8 lists the relationship between slenderness ratio and stability coefficient φ of all the specimens in this test. With the growth of the slenderness ratio, the stability coefficient φ gradually decreased. There is eccentric moment because of the initial imperfection. When the slenderness ratio is larger, the lateral displacement of the column middle part is greater, which produces the larger moment. It makes components damaged more easily. It is same with the other materials.

The specimens of group SC-2 and SC-3 have the same section parameters except the concrete strength. Compared with the results of two groups in Figure 8, the stability coefficient ϕ of SC-2 with higher core concrete strength is larger than that of SC-3. But for the normal CFST, Cai (2003) believes that the concrete strength has no obvious impact on the stability coefficient [13], while Han (2004) believes it has impact [14]. The reasons will be discussed later.

The confinement coefficient ζ influences the behavior of short CFST columns. But for SC-1, SC-2 and SC-3, the confinement coefficient is more and more low. Especially for group SC1 and SC3, the specimens have the same concrete strength, but with different confinement coefficient ζ . And there is no obvious variation of ϕ as ζ increasing with the parameter range in this test (Figure 8).

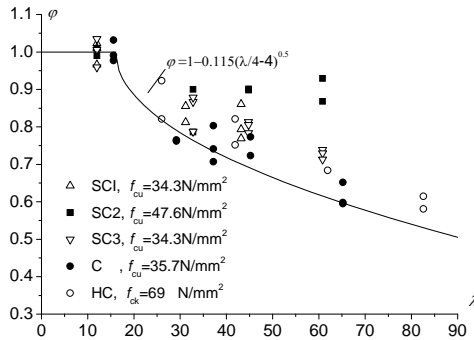


Figure 8. $\phi - \lambda$ Relation

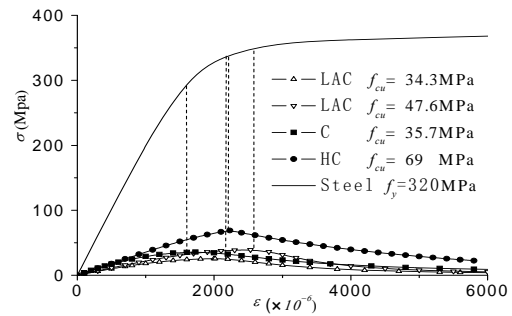


Figure 9. $\sigma - \epsilon$ Relation of Different Concrete

4.2 Influence Mechanism Analysis

Core concrete not only delays the occurrence of steel local buckling, but also bears pressure. When the local strain of concrete filled steel tube specimens is larger than ultimate strain of the concrete, the concrete in near position goes into the plastic state and the load bearing by steel tube increases rapidly. Then the steel is yielded and specimen is damaged. The performances of concrete influence the mechanical behavior of specimens.

In Figure 8, the stability coefficient ϕ of LACFST in this test and normal CFST tested by other researchers are listed. The empirical formula curve of normal CFST [13] is drawn in the figure too. Group C represents normal concrete, and group HC represents high strength concrete [13]. The stability coefficient results of LACFST are all above on the curve of empirical formula. Comparison from the figure, the following order can be got.

$$\phi_{LAC47.6} > \phi_{LAC34.3} \approx \phi_{HC69} > \phi_{C35.7} \tag{3}$$

Relation formula above shows that higher concrete strength does not mean higher stability coefficient. As an important indicator of concrete strength, f_{cu} has no influence to the stability coefficient of CFST.

The properties of confined concrete influence by the unconfined concrete properties and constraint force mainly. And ζ is the main reflection to the constraint force. Because there is no obvious variation of ϕ as ζ increasing in this test which is get from above analysis. So the influence to stability coefficient of the confined concrete can mainly been reflected by unconfined concrete properties. Figure 9 shows the stress-strain curves of steel and four kinds concrete. The curve of steel is obtained from the test. The curves of concrete are calculated by the unconfined concrete methods suggested in literature [15, 16]. Comparison from the figure, the following order of peak strain can be got. It has same variation regularity with the stability coefficient ϕ .

$$\varepsilon_{LAC47.6} > \varepsilon_{LAC34.3} \approx \varepsilon_{HC69} > \varepsilon_{C35.7} \quad (4)$$

Compare to the curves of steel and concrete in Figure 9, the peak strain of the normal concrete appears before the steel's. When the normal concrete goes into elastic-plastic state, the steel is also in the elastic state. Although the bearing capacity of normal concrete decreases, it will be compensated by the steel. So the specimen bearing capacity also increases slowly. The specimen damages after the steel going into the elastic-plastic state. In this case, stability bearing capacity of specimen is determined by the behavior of steel. But it is influenced by the peak strain of concrete actually.

But the peak strain of the lightweight aggregate concrete appearances after the steel's. The steel goes into elastic-plastic state before LAC. When the bearing capacity of LAC decreased, the steel can't compensate it. The specimen damages after reaching to the peak strain of LAC. In this case, stability bearing capacity of specimen is determined by the peak strain of LAC.

The peak strain of high strength concrete ($f_{cu}=69\text{MPa}$) is almost equal to that of LAC ($f_{cu}=34.3\text{MPa}$). And stability coefficient of high strength concrete ($f_{cu}=69\text{MPa}$) is also almost equal to that of LAC ($f_{cu}=34.3\text{MPa}$). Compare to the order of stability coefficient and concrete peak strain, they are same. So the larger peak strain of LAC is, the larger stability bearing capacity and coefficient of specimens are. It can be concluded that the stability coefficient of specimens are determined by the peak strain of concrete with the studied scope of parameters in this paper.

5. BEARING CAPACITY CALCULATION

There are no existing methods to calculate the bearing capacity of lightweight aggregate concrete filled steel tube. But for the normal concrete filled steel tube, different formulas are suggested in some country or region national codes. In this paper, three methods suggested for normal concrete filled steel tube are used to calculate the bearing capacity of specimens in this test, concluding AISC-LRFD(United States), EC4(Europe) and CECS28:90(China). The calculation results are listed in Table 4. It is compared with the test results. In Table 4, N_u is test ultimate bearing capacity, N_{uc} is calculation ultimate bearing capacity. And Figure 10 is used to show the comparison results more clearly.

Table 4. Bearing Capacity Calculation

Specimen number	λ	Test $N_u(\text{kN})$	AISC-LRFD(99)		EC4(1996)		CECS28:90(1992)	
			$N_{uc}(\text{kN})$	N_{uc}/N_u	$N_{uc}(\text{kN})$	N_{uc}/N_u	$N_{uc}(\text{kN})$	N_{uc}/N_u
SC1-7-a	31.2	793.33	615.05	0.775	838.21	1.057	811.21	1.023
SC1-7-b	31.2	753.33	615.05	0.816	838.21	1.113	811.21	1.077
SC1-10-a	43.2	798.10	605.23	0.758	798.84	1.001	732.05	0.917
SC1-10-b	43.2	713.33	605.23	0.848	798.84	1.120	732.05	1.026
SC1-10-c	43.2	736.19	605.23	0.822	798.84	1.085	732.05	0.994
SC2-7-a	32.8	799.05	559.66	0.700	757.31	0.948	830.80	1.040
SC2-7-b	32.8	698.10	559.66	0.802	757.31	1.085	830.80	1.190
SC2-10-a	44.8	797.14	548.27	0.688	716.18	0.898	751.56	0.943
SC2-10-c	44.8	800.00	548.27	0.685	716.18	0.895	751.56	0.939
SC2-14-a	60.8	824.76	527.45	0.640	645.50	0.783	668.64	0.811
SC2-14-b	60.8	770.48	527.45	0.685	645.50	0.838	668.64	0.868

SC3-7-a	32.8	584.76	451.30	0.772	623.17	1.066	594.60	1.017
SC3-7-b	32.8	643.81	451.30	0.701	623.17	0.968	594.60	0.924
SC3-7-c	32.8	652.38	451.30	0.692	623.17	0.955	594.60	0.911
SC3-10-a	44.8	603.81	441.37	0.731	595.00	0.985	537.89	0.891
SC3-10-b	44.8	598.10	441.37	0.738	595.00	0.995	537.89	0.899
SC3-10-c	44.8	581.90	441.37	0.758	595.00	1.023	537.89	0.924
SC3-14-a	60.8	548.57	423.26	0.772	547.94	0.999	478.54	0.872
SC3-14-b	60.8	541.90	423.26	0.781	547.94	1.011	478.54	0.883
SC3-14-c	60.8	529.52	423.26	0.799	547.94	1.035	478.54	0.904
AVERAGE (μ)				0.748		0.992		0.953
SD (δ)				0.055		0.087		0.086

From Table 4 and Figure 10, the results of AISC-LRFD (1999) are the safest one, and the results of EC4 (1996) and CECS28:90(1992) approach to the test ones. But the deviation of CECS28:90(1992) is greater than that of EC4 (1996) when the specimen has a large slenderness. For the results of EC4 (1996), the average is 0.992, and the standard deviation is 0.087. It is closest to the test results and has a low discreteness. It can be used to calculate the bearing capacity of LACFST long columns. Based on the calculation using EC4 (1996) to the LACFST short columns bearing capacity, the average value is 1.077, and the standard deviation is 0.053. The formula in EC4 (1996) also has a preferable goodness of fit to calculate the bearing capacity of short columns. So it can be concluded that the calculation method in EC4 (1996) can be suggested to calculate the bearing capacity of LACFST under axial compression.

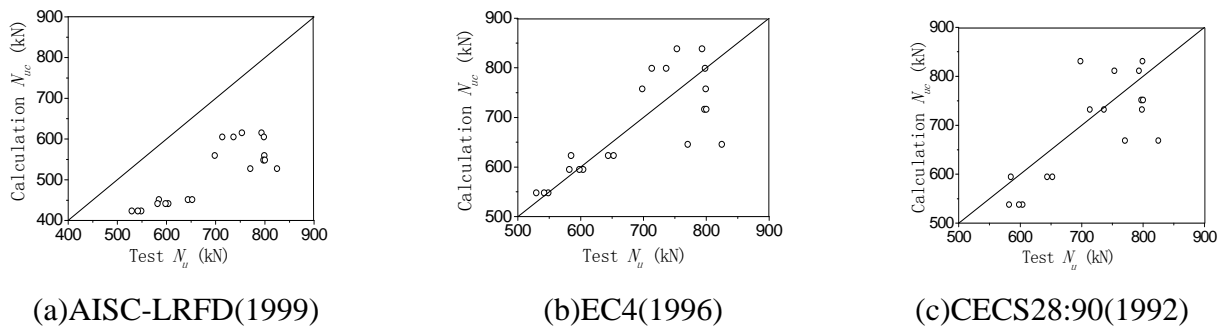


Figure 10. Test and Calculation Bearing Capacity Results Comparison

6. CONCLUSIONS

- (1) Slenderness ratio is very important influence parameters to the behavior of lightweight aggregate concrete filled steel tube slender columns under axial compressive load. With the same other section parameters, the greater the slenderness ratio is, the lower the ultimate bearing capacity of the specimen is and the worse the plastic deformation capacity is. The stability coefficient decreases as the increasing of slenderness ratio.

- (2) The performances of core concrete influence the stability behavior of lightweight aggregate concrete filled steel tube and normal concrete filled steel tube columns. The stability coefficient of specimens is determined by the peak strain of concrete and the peak strength of concrete has no influence to stability coefficient. The stability coefficient increases when the peak strain of concrete increases. Because of the larger peak strain of concrete, the stability coefficient of specimens with higher strength is higher than that of core concrete with lower strength in this test.
- (3) Based on the comparison of bearing capacity calculation using different methods, calculation formula in Europe code EC4 (1996) can be suggested to calculate the bearing capacity of lightweight aggregate concrete filled steel tube columns axial compression. The calculation results have a preferable goodness of fit to the test ones in this paper.

ACKNOWLEDGMENTS

The authors appreciate the support of Natural Science Foundation of Jiangsu Province, The Fundamental Research Funds for the Central Universities, and Jiangsu Civil Engineering Graduate Center for Innovation and Academic Communication foundation.

REFERENCES

- [1] Ge, H.B., Susantha, K.A.S., Satake, Y., et al., "Seismic Demand Predictions of Concrete-filled Steel Box Columns", *Engineering Structures*, 2003, Vol. 25, No. 3, pp. 337-345.
- [2] Han, L.H., Lu, H., Yao, G.H., et al., "Further Study on the Flexural Behaviour of Concrete-filled Steel Tubes", *Journal of Constructional Steel Research*, 2006, Vol. 62, No. 6, pp. 554-565.
- [3] Kuranovas, A., Goode, D., Kvedaras, A.K., et al., "Load-bearing Capacity of Concrete-filled Steel Columns", *Journal of Civil Engineering and Management*, 2009, Vol. 15, No. 1, pp. 21-33.
- [4] Gao, S.B. and Ge, H.B., "Numerical Simulation of Hollow and Concrete-filled Steel Columns", *Int. J. of Advanced Steel Construction*, Vol. 3, No. 3, pp. 668-678.
- [5] Goode, C.D., "Composite Columns - 1819 Tests on Concrete-filled Steel Tube Columns Compared with Euro Code 4", *Structural Engineer*, 2008, Vol. 86, No. 16, pp. 33-38.
- [6] Chen, B.C. and Wang, T.L., "Overview of Concrete Filled Steel Tube Arch Bridges in China", *Practice Periodical on Structural Design and Construction*, 2009, Vol. 14, No. 2, pp. 70-80.
- [7] Susantha, K.A.S., Ge, H.B. and Usami, T., "Cyclic Analysis and Capacity Prediction of Concrete-filled Steel Box Columns", *Earthquake Engineering & Structural Dynamics*, 2002, Vol. 31, No. 2, pp. 195-216.
- [8] Ge, H.B. and Usami, T. "Cyclic Tests of Concrete-filled Steel Box Columns", *Journal of Structural Engineering*, ASCE, 1996, Vol. 122, No. 10, pp. 1169-1177.
- [9] Liu, H.Y. and Song, Y.P., "Experimental Study of Lightweight Aggregate Concrete under Multiaxial Stresses", *Journal of Zhejiang University-Science A*, 2010, Vol. 11, No. 8, pp. 545-554.
- [10] Haque, M.N., Al-Khaiat, H. and Kayali, O., "Strength and Durability of Lightweight Concrete", *Cement and Concrete Composites*, 2004, Vol. 26, No. 4, pp. 307-314.

- [11] Nakamura, S., Momiyama, Y., Hosaka, T., et al., “New Technologies of Steel/Concrete Composite Bridges”, *Journal of Constructional Steel Research*, 2002, Vol. 58, No. 1, pp. 99-130.
- [12] Mouli, M. and Khelafi, H., “Strength of Short Composite Rectangular Hollow Section Columns Filled with Lightweight Aggregate Concrete”, *Engineering Structures*, 2007, Vol. 29, No. 8, pp. 1791-1797.
- [13] Cai, S.H., “Modern Concrete Filled Steel Tube Structure”, China Communications Press, 2003, pp. 63 (in Chinese).
- [14] Han, L.H. and Yang, Y.F., “Modern Concrete Filled Steel Tube Structure Technology”, China Architecture & Building Press, 2004, pp. 80 (in Chinese).
- [15] Wang, Z.Y., Ding, J.T. and Guo, Y.S., “Stress-Strain Curves of Structural Lightweight Aggregate Concretes”, *Concrete*, 2005, No. 3, pp. 39-41 (in Chinese).
- [16] Chinese Code, “Code for Design of Concrete Structures (GB 50010-2002)”, 2002 (in Chinese).